

Lateral Casimir force beyond the Proximity Force Approximation

Robson B. Rodrigues,¹ Paulo A. Maia Neto,¹ Astrid Lambrecht,² and Serge Reynaud²

¹*Instituto de Física, UFRJ, CP 68528, Rio de Janeiro, RJ, 21941-972, Brazil*

²*Laboratoire Kastler Brossel, CNRS, ENS, Université Pierre et Marie Curie case 74, Campus Jussieu, F-75252 Paris Cedex 05, France*

(Dated: July 13, 2018)

We argue that the appropriate variable to study a non trivial geometry dependence of the Casimir force is the lateral component of the Casimir force, which we evaluate between two corrugated metallic plates outside the validity of the Proximity Force Approximation (PFA). The metallic plates are described by the plasma model, with arbitrary values for the plasma wavelength, the plate separation and the corrugation period, the corrugation amplitude remaining the smallest length scale. Our analysis shows that in realistic experimental situations the Proximity Force Approximation overestimates the force by up to 30%.

Considerable experimental progress has been achieved [1] in the measurement of the Casimir force, opening the way for various applications in nano-science [2], particularly in the development of nano- or micro-electromechanical systems (NEMS or MEMS). Calculations are much simpler in the original Casimir geometry of two plane plates [3] which obeys a symmetry with respect to lateral translations and thus allows to derive the expression of the Casimir force from the reflection amplitudes which describe specular scattering on the plates [4].

More general geometries open a far richer physics with a variety of extremely interesting theoretical predictions [5]. Up to now the experimental studies of the effect of geometry have been restricted to simple configurations which can be calculated with the help of the Proximity Force Approximation (PFA). This approximation is essentially equivalent to an averaging over plane-plane geometries and its result can be deduced from the force known in this geometry [6]. For example, it allows to evaluate the force between a plane and a sphere [7] provided the radius R of the sphere is much larger than the mirror separation $R \gg L$. It is also valid for the description of the effect of roughness when the wavelengths associated with the plate deformations are large enough [8]. However PFA relies heavily on assuming some additivity of Casimir forces which is known to be generally not valid except for very smooth geometrical perturbations [9].

The aim of the present paper is to study a configuration allowing a new test of QED theoretical predictions outside the PFA domain and independent of those already performed in the plane-plane geometry. The idea is to look for the lateral component of the Casimir force which appears, besides the usual normal component, when periodic corrugations with the same period are imprinted on the two metallic plates. This configuration contrasts with other ones, for example the normal Casimir force in the plane-sphere geometry or roughness corrections to it. There PFA can also be invalid, but this leads only to small corrections of the dominant normal Casimir force, which do not seem accessible experimentally at the moment. The lateral component of the

Casimir force has recently been measured and analyzed within the PFA [10, 11]. We find for experimentally realizable parameters that PFA overestimates the force by as much as 30%, which should allow for a rapid experimental check of its validity.

The lateral Casimir force between corrugated surfaces has been analyzed outside the PFA domain for perfect reflectors [12] where interesting results were obtained for arbitrary values of the ratio λ_C/L of the corrugation wavelength λ_C to the interplate distance L . However, the assumption of perfect reflections can only be valid in the limit of large distances where the lateral force tends to become too weak to be measurable. Experimental conditions allowing the lateral force to be measured correspond to separations of a few hundred nanometers [10], that is of the same order of magnitude as the plasma wavelength λ_P associated with the metallic plates, so that they cannot be treated even as approximately perfect reflectors [13]. In contrast, the calculations presented here allow to predict the lateral force in this domain.

In this letter, we calculate the lateral force for metallic plates modeled by the plasma model with arbitrary values of L , λ_C and λ_P . We use the perturbative approach that we developed for analyzing the effect of stochastic roughness on the normal Casimir force [14, 15]. This technique is valid as long as the corrugation amplitude a remains the smallest of length scales $a \ll L, \lambda_C, \lambda_P$. As this condition does not depend on the relative magnitudes of the three other length scales, it allows us to study situations beyond the PFA where the lateral force is experimentally accessible. The result will be expressed in terms of a non linear susceptibility function, calculated from non-specular scattering amplitudes [16] associated with corrugated metallic surfaces. This function, obtained within the scattering approach [17], can itself be considered as a new QED theoretical prediction to be compared with forthcoming experiments.

The surface profiles of the two parallel corrugated plates are defined by two functions $h_1(\mathbf{r})$ and $h_2(\mathbf{r})$, with $\mathbf{r} = (x, y)$ the lateral position along the surfaces of the plates. Both distributions h_1 and h_2 have zero spatial averages $\langle h_j \rangle = 0, j = 1, 2$, and they are counted as

positive when they correspond to local length decreases below the mean value L . The corrugated surfaces are assumed to be static, so that the field frequency ω is preserved by scattering. In contrast, the lateral wavevector components $\mathbf{k} = (k_x, k_y)$ as well as the polarization of the field are modified. Scattering on the plate $j = 1, 2$ is thus described by non-specular reflection amplitudes $\mathcal{R}_{j;pp'}(\mathbf{k}, \mathbf{k}', \omega)$, where \mathbf{k}, \mathbf{k}' represent the lateral wavevectors of the input and output fields and p and p' their polarizations, TE for transverse electric and TM for transverse magnetic (more detailed definitions in [14, 15]).

For the purpose of the present paper, the non-specular reflection amplitudes have to be developed up to the first order in the deviations h_j from flatness of the two plates

$$\begin{aligned} \mathcal{R}_{j;pp'}(\mathbf{k}, \mathbf{k}', \omega) &= (2\pi)^2 \delta^{(2)}(\mathbf{k} - \mathbf{k}') \delta_{pp'} r_{j;p}(\mathbf{k}, \omega) \\ &+ R_{j;pp'}(\mathbf{k}, \mathbf{k}'; \omega) H_j(\mathbf{k} - \mathbf{k}') \end{aligned} \quad (1)$$

The first line in this equation represents the zero-th order term with respect to corrugation, that is also the specular reflection on a flat plate (with $r_{j;p}(\mathbf{k}, \omega)$ the ordinary specular reflection amplitude [17]). The second line describes the first-order correction proportional to the Fourier component $H_j(\mathbf{k} - \mathbf{k}')$ of the profiles $h_j(\mathbf{r})$, this Fourier component being able to induce a modification of the field wavevector from \mathbf{k} to \mathbf{k}' .

We then compute the correction of the Casimir energy δE_{PP} induced by the corrugations. At the lowest order, we have to use the scattering approach [15] at second order in the corrugations, keeping only the crossed terms of the form $H_1 H_2$ which have the ability to induce lateral forces. This means that the sensitivity function obtained below depends on the crossed correlation between the profiles of the two plates, in contrast to the function which was calculated for describing roughness correction in [14, 15]. The latter were depending on terms quadratic in H_1 or H_2 , and their evaluation required that second order non specular scattering be properly taken into account. Here, first order non specular amplitudes evaluated on both plates are sufficient.

Assuming for simplicity that the two plates are made of the same metallic medium, so that explicit reference to the index j may be omitted in the reflection amplitudes from now on (otherwise the result is given by a trivial extension), we obtain the second-order correction

$$\delta E_{\text{PP}} = \int \frac{d^2 \mathbf{k}}{(2\pi)^2} \mathcal{G}(\mathbf{k}) H_1(\mathbf{k}) H_2(-\mathbf{k}) \quad (2)$$

The non linear response function $\mathcal{G}(\mathbf{k})$ is given by

$$\begin{aligned} \mathcal{G}(\mathbf{k}) &= -\hbar \int_0^\infty \frac{d\xi}{2\pi} \int \frac{d^2 \mathbf{k}'}{(2\pi)^2} b_{\mathbf{k}', \mathbf{k} - \mathbf{k}}(\xi) \\ b_{\mathbf{k}', \mathbf{k}} &= \sum_{p', p} \frac{e^{-(\kappa' + \kappa)L} R_{p'p}(\mathbf{k}', \mathbf{k}; \xi) R_{pp'}(\mathbf{k}, \mathbf{k}'; \xi)}{(1 - r_{p'}(\mathbf{k}')^2 e^{-2\kappa' L}) (1 - r_p(\mathbf{k})^2 e^{-2\kappa L})} \end{aligned} \quad (3)$$

Note that the integral over real frequencies ω has been replaced by an integral over imaginary frequencies ξ , while

the round-trip propagation factor between the plates is now expressed as $\exp(-2\kappa L)$, with $\kappa = \sqrt{k^2 + \xi^2/c^2}$. For isotropic media, symmetry requires the response function $\mathcal{G}(\mathbf{k})$ to depend only on the modulus $k = |\mathbf{k}|$.

Experiments with corrugated plates [10] were corresponding to the simple case where uniaxial sinusoidal corrugations are imprinted on the two plates along the same direction, say the y direction, and with the same wavevector $k \equiv 2\pi/\lambda_C$

$$h_1 = a_1 \cos(kx) \quad , \quad h_2 = a_2 \cos(k(x+b)) \quad (4)$$

The energy correction thus depends on the lateral mismatch b between the corrugations of the two plates, which is the cause for the lateral force to arise. Replacing the ill-defined $(2\pi)^2 \delta^{(2)}(0)$ by the area A of the plates, we derive from (2)

$$\delta E_{\text{PP}} = A \frac{a_1 a_2}{2} \cos(kb) \mathcal{G}(k) \quad (5)$$

The result of the PFA can be recovered from Eq. (5) as the limiting case $k \rightarrow 0$. PFA indeed correspond to long corrugation wavelengths, that is also nearly plane surfaces so that the Casimir energy is obtained from the plane-plane energy $E_{\text{PP}}(z)$ by averaging the ‘local’ distance $z = L - h_1 - h_2$ over the surface of the plates [9]. Expanding at second order in the corrugations, we thus obtain the following dependence of the energy (as before we disregard terms in a_1^2 and a_2^2 because they do not depend on the relative lateral position)

$$\delta E_{\text{PP}} = \frac{a_1 a_2}{2} \cos(kb) \frac{d^2 E_{\text{PP}}}{dz^2} \quad , \quad [\text{PFA}] \quad (6)$$

This reproduces (5) for large values of λ_C because the response function $\mathcal{G}(k)$ satisfies the condition

$$\lim_{k \rightarrow 0} A \mathcal{G}(k) = \frac{d^2 E_{\text{PP}}}{dz^2} \quad (7)$$

This property is ensured, for any specific model of the material medium, by the fact that \mathcal{G} is given for $k \rightarrow 0$ by the specular limit of non specular reflection amplitudes (more details in [15]). For arbitrary values of k , the deviation from PFA is described by the ratio

$$\rho(k) = \frac{\mathcal{G}(k)}{\mathcal{G}(0)} \quad , \quad \lim_{k \rightarrow 0} \rho(k) = 1 \quad (8)$$

In the following, we discuss explicit expressions of this ratio ρ obtained from the general result (3) in the particular case of metallic mirrors described by the plasma model. The dielectric function is thus given by $\epsilon = 1 + \omega_{\text{P}}^2/\xi^2$, with the plasma wavelength and frequency related by $\lambda_{\text{P}} = 2\pi c/\omega_{\text{P}}$. For the numerical examples, we will take $\lambda_{\text{P}} = 136\text{nm}$, corresponding to gold covered plates. The non-specular coefficients appearing in Eq. (3) are then evaluated from Ref. [15]. The resulting function ρ is plotted on Fig. 1 as a function of k , for different values of the separation distance L .

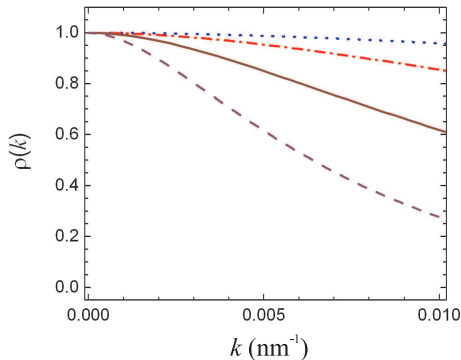


FIG. 1: Variation of ρ versus k with $\lambda_P = 136\text{nm}$ and for $L = 50\text{nm}$ (dotted line), 100nm (dash-dotted line), 200nm (solid line) and 400nm (dashed line).

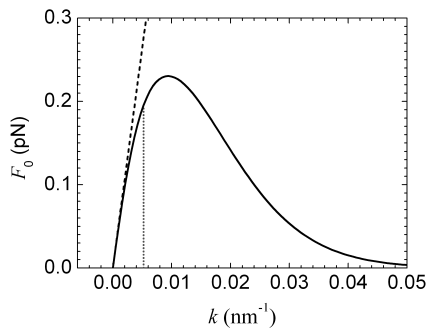


FIG. 2: Lateral force amplitude for the plane-sphere setup, as a function of k , with figures taken from [10]. The experimental value $k = 0.0052\text{nm}^{-1}$ is indicated by the vertical dashed line.

As expected, the PFA ($\rho = 1$) is a better approximation at short distances. For $L = 50\text{nm}$ for example, the approximation is correct in the range $k \leq 0.01\text{nm}^{-1}$ (*i.e.* $\lambda_C \geq 628\text{nm}$) covered by the plot in Fig. 1. For larger distances, PFA is found to *overestimate* the energy correction and, therefore, the lateral force. For parameters $L = 200\text{nm}$ and $\lambda_C = 1.2\mu\text{m}$ ($k = 0.0052\text{nm}^{-1}$) close to the experimental figures of Ref. [10], we find the lateral force smaller by a factor $\rho = 0.84$. In other words, the correction expected with respect to PFA calculations is of the order of 16%.

For still larger values of k , the functions $\mathcal{G}(k)$ and $\rho(k)$ decay exponentially to zero. When the momentum transfer k is much larger than $1/L$, the function $b_{\mathbf{k}', \mathbf{k} - \mathbf{k}}$ in Eq. (3) is proportional to the exponentially small factor $\exp(-kL)$. If we also assume that $k\lambda_P \gg 1$, we find $\mathcal{G}(k) = \alpha k \exp(-kL)$ where the parameter α now depends on λ_P and L only. This is in striking contrast with the behavior of the response function for stochastic roughness, which *grows* linearly with k for large k due to the contribution of the second-order reflection coefficients [15]. These coefficients do not contribute to the second-

order lateral effect, which is related to two first-order non-specular reflections at different plates, separated by a one-way propagation with a modified momentum of the order of k . The resulting propagation factor is, in the large- k limit, $\exp(-\kappa L) \approx \exp(-kL)$, thus explaining the exponential behavior.

For intermediate values of k , $\mathcal{G}(k)$ is also smaller than the roughness response function, although no simple analytical expression is available in the general case. Thus, the exact calculation decreases the PFA value for the lateral effect, in contrast to the case of stochastic roughness correction where they increase the PFA value [14, 15].

We now compare the theoretical expression of the lateral Casimir force to realistic experiments and therefore consider the plane-sphere (PS) geometry [10] rather than the plane-plane (PP) geometry as before. The PS result can be derived from the PP one by using PFA with validity conditions more easily met than those which would be necessary for computing the corrugation effect. As a matter of fact, PFA may account for the curvature of the sphere as soon as the radius R of the sphere is larger than the distance $R \gg L$. Then any interplay between curvature and corrugation is avoided provided that $RL \gg \lambda_C^2$. These two conditions are met in the experiment reported in [10], where $R = 100\mu\text{m}$, $\lambda_C = 1.2\mu\text{m}$ and $L \sim 200\text{nm}$. PFA is likely a very good approximation as far as curvature is concerned whereas, for the corrugation effect itself, a deviation from the PFA is expected since L is not so much smaller than λ_C .

Applying the PFA to describe the PS configuration, we obtain the energy correction δE_{PS} between the sphere and a plane at a distance of closest approach L as an integral of the energy correction δE_{PP} in the PP geometry

$$\delta E_{PS}(L, b) = \int_{\infty}^L \frac{2\pi R dL'}{A} \delta E_{PP}(L', b) \quad (9)$$

Then the lateral force is deduced by varying the energy correction with respect to the lateral mismatch b between the two corrugations. This gives the lateral Casimir force in the PS geometry as an average of

$$F_{PS}^{\text{lat}}(L, b) \equiv -\frac{\partial}{\partial b} E_{PS}(L, b) = \int_{\infty}^L \frac{2\pi R dL'}{A} F_{PP}^{\text{lat}}(L', b) \quad (10)$$

$$F_{PP}^{\text{lat}}(L, b) \equiv -\frac{\partial}{\partial b} E_{PP}(L, b)$$

leading eventually with Eq. (5) to

$$F_{PS}^{\text{lat}} = \pi a_1 a_2 k R \sin(kb) \int_{\infty}^L dL' \mathcal{G}(k, L') \quad (11)$$

The force attains a maximal amplitude for $\sin(kb) = \pm 1$, which is easily evaluated in the PFA regime $k \rightarrow 0$ where $\mathcal{G}(k)$ does not depend on k , so that F_{PS}^{lat} scales as k . However, as k increases, the amplitude increases at a slower rate and then starts to decrease due to the exponential decay of $\mathcal{G}(k)$. Thus, for a given value of the separation

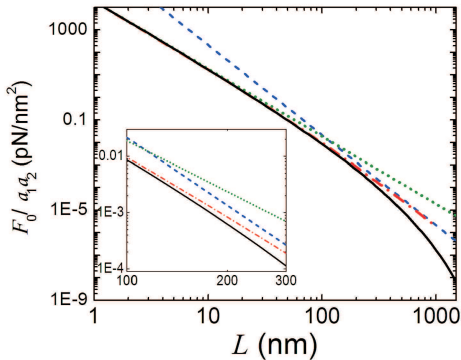


FIG. 3: Plane-sphere geometry: $F_{\text{PS}}^{\text{lat}}/(a_1 a_2 \sin(kb))$ as a function of L , with $k = 0.0052 \text{nm}^{-1}$. The solid line is the exact result obtained in this paper. Other lines represent various approximations: PFA (dotted-dashed) and PFA combined with the perfectly-reflecting (dashed) and plasmon (dotted) limits.

L , the lateral force reaches an optimum for a corrugation wavelength such that kL is of order of unity, which generalizes the result obtained for perfect reflectors in [12]. In Fig. 2, we plot the force $F_{\text{PS}}^{\text{lat}}$ (for $\sin(kb) = 1$) as a function of k , with figures taken from the experiment of Ref. [10]. We also use the values $a_1 = 59 \text{nm}$ and $a_2 = 8 \text{nm}$ of the amplitudes for measuring the force as in [10], reminding however that our calculations are valid in the perturbative limit $a_1, a_2 \rightarrow 0$.

The plot clearly shows the linear growth for small k as well as the exponential decay for large k . The maximum force is at $k = 0.009 \text{nm}^{-1}$ so that $kL \simeq 2$. The experimental value $k = 0.0052 \text{nm}^{-1}$ is indicated by the dashed line in Fig. 2, and the force obtained as 0.20pN , well below the PFA result, indicated by the straight line and corresponding to a force of 0.28pN . This last value

is very close to the number calculated by Ref. [10], if we discount the correction due to higher order terms beyond the second order approximation considered in the present paper. Precisely, Ref. [10] finds a force of 0.32pN at $L = 221 \text{nm}$, with a relative correction due to higher powers of 1.21 . Discounting this factor, the second-order force should be 0.26pN , which overestimates the exact result by a factor of the order of 30%.

In order to discuss the dependence of the force versus the distance L , we plot $F_{\text{PS}}^{\text{lat}}/(a_1 a_2 \sin(kb))$ with log-log scales on Fig. 3, with $\lambda_C = 1.2 \mu\text{m}$ (solid line). For very small values of L , we find the L^{-3} power law expected for the plasmon limit $L \ll \lambda_P$ [18] combined with PFA (dotted line). We also show the PFA result for arbitrary λ_P/L (dotted-dashed line) and the $1/L^4$ dependence resulting from the combination of PFA and perfectly-reflecting assumption (dashed line). Fitting in the range between 150 and 300 nm, we find the power law $L^{-4.1}$, in agreement with the experimental result [10]. But Fig. 3 shows that the force decays faster for larger values of L , leading ultimately to an exponential decay.

These results indicate the way to be followed to perform an accurate comparison between theory and experiment in a configuration where geometry plays a non trivial role, *i.e.* beyond the PFA. Such a comparison should be pursued by looking at the lateral force between corrugated metallic plates. This problem can neither be addressed by calculations performed with the help of PFA [10, 11], nor with the assumption of perfect reflection [12]. But it can be tackled by the technique presented in the present letter which is valid for arbitrary relative values of L , λ_C and λ_P , provided that the corrugation amplitude is smaller than the other length scales.

One of us (P. A. M. N.) thanks CNPq and Instituto do Milênio de Informação Quântica for partial financial support.

-
- [1] A. Lambrecht and S. Reynaud, in *Poincaré Seminar 2002 'Vacuum Energy'*, ed. B. Duplantier and V. Rivasseau (Birkhäuser, 2003), p. 109 and references therein; F. Chen *et al*, Phys. Rev. A **69** 022117 (2004); R.S. Decca *et al*, Annals Phys. **318** 37 (2005).
 - [2] H.B. Chan *et al*, Science **291** 1941 (2001).
 - [3] H.B.G. Casimir, Proc. K. Ned. Akad. Wet. **51** 793 (1948).
 - [4] M.-T. Jaekel and S. Reynaud, J. Physique **I-1**, 1395 (1991).
 - [5] R. Balian and B. Duplantier, Proc. of the 15 th SIGRAV Conference on Gen. Rel. and Grav. Physics (2004) [preprint quant-ph/0408124] and references therein.
 - [6] B.V. Deriagin, Kolloid Z. **69**, 155 (1934).
 - [7] R.L. Jaffe and A. Scardicchio, Phys. Rev. Lett. **92** 070402 (2004).
 - [8] G.L. Klimchitskaya *et al*, Phys. Rev. **A60**, 3487 (1999).
 - [9] C. Genet *et al*, Europhys. Lett. **62** 484 (2003).
 - [10] F. Chen *et al*, Phys. Rev. Lett. **88**, 101801 (2002); Phys. Rev. A **66**, 032113 (2002).
 - [11] E.V. Blagov *et al*, Phys. Rev. A. **69**, 044103 (2004).
 - [12] T. Emig *et al*, Phys. Rev. A **67**, 022114 (2003); T. Emig, Europhys.Lett. **62** 466 (2003).
 - [13] A. Lambrecht and S. Reynaud, Eur. Phys. J. **D8** 309 (2000).
 - [14] P.A. Maia Neto, A. Lambrecht and S. Reynaud, Europhys. Lett. **69**, 924 (2005).
 - [15] P.A. Maia Neto, A. Lambrecht and S. Reynaud, Phys. Rev. A **72**, 012115 (2005).
 - [16] A.A. Maradudin and D.L. Mills, Phys. Rev. B **11**, 1392 (1975); G.S. Agarwal, Phys. Rev. B **15**, 2371 (1977); J.-J. Greffet, Phys. Rev. B **37**, 6436 (1988); J. Sanchez-Gil and M. Nieto-Vesperinas, J. Opt. Soc. Am. A **8**, 1270 (1991).
 - [17] C. Genet, A. Lambrecht and S. Reynaud, Phys. Rev. A **67**, 043811 (2003).
 - [18] F. Intravaia and A. Lambrecht, Phys. Rev. Lett. **94**, 110404 (2005).